K-Band Integrated Double-Balanced Mixer

HIROYO OGAWA, MASAYOSHI AIKAWA, MEMBER, IEEE, AND KOZO MORITA

***Abstract*—A novel microwave integrated circuit (MIC) double-balanced mixer with good isolation between the three ports is described. The mixer is fabricated using a combination of microstrip lines, slotlines, and coupled slotlines, together with four beam-lead Schottky-barrier diodes. The *K*-band magic-T has been developed for the double-balanced mixer. The minimum conversion loss measured at a signal frequency of 19.6 GHz is 4.7 dB. Isolation between RF and LO ports is greater than 20 dB from 18 to 21 GHz. The mixer can be expected to have wide applications in MIC receivers and transmitters up to the millimeter-wave band.**

I. Introduction

RECENTLY, microwave integrated circuit (MIC) balanced mixers have been produced for use in high-frequency bands [1]–[8]. Balanced-type mixers have several desirable features, such as good isolation and suppression of undesired signals. Though the hybrid circuits are easily fabricated on a dielectric substrate, the MIC high-Q filters which are needed for an unbalanced-type mixer cannot be easily fabricated for the millimeter-wave band. Consequently, the balanced-type mixer which does not require filters is suitable for MIC's in high-frequency bands.

MIC balanced mixers have been constructed using combinations of microstrip lines, slotlines, and coplanar lines. In particular, the cascade connection of slotlines and coplanar lines has recently been used for single-balanced mixers [3]–[7]. Four-port hybrid circuit have also been used for single-balanced mixers. Double-balanced mixers are not easily fabricated in high-frequency bands because of the complexity of their circuit configuration as compared with unbalanced or single balanced mixers.

In this paper, a new structure for a double-balanced mixer is proposed using a combination of microstrip lines, slotlines and coupled slotlines. Slotlines are employed as the main MIC transmission line. The mixer is composed of an MIC magic-T (180° hybrid), and a diode circuit with four beam-lead Schottky-barrier diodes. The magic-T is developed for *K*-band [9], [10] and is an essential part of the double-balanced mixer. Since this magic-T has a four-port configuration different from that of the conventional 180° hybrid, it is possible to construct a double-balanced mixer with no crossing of transmission lines. The high directivity of the magic-T will only result in good isolation in the mixer if the diodes and diode circuits are also well-matched to one-another. The diode circuit consists of slotlines, microstrip lines and four beam-lead diodes, and has low coupling of even LO harmonics to the RF input. The harmonic sidebands of $mf_{LO} \pm f_{RF}$ (m = an odd integer) are obtained at the IF signal port. This paper describes the circuit configuration, the basic behavior of the mixer using its equivalent circuit and the experimental results obtained in the 20-GHz band.

Manuscript received July 30, 1979; revised October 15, 1979.

The authors are with the Radio Transmission Section, Yokosuka Electrical Communication Laboratories, Nippon Telegraph and Telephone Public Corporation, Yokosuka, 238-03 Japan.

II. Circuit Configuration

The configuration of the double-balanced mixer is shown in Fig. 1. This circuit is composed of an MIC magic-T and a diode circuit. In this figure, solid lines indicate slotlines and coupled slotlines on the substrate, while dotted lines indicate microstrip lines on the reverse side of the substrate. Two circular marks "o" indicate cylindrical conductors used for connecting slotlines and microstrip lines through holes in the substrate. Ⓡ, Ⓛ, and Ⓘ denote RF input port, LO input port, and IF output port, respectively.

The RF and LO signals are fed into ports Ⓡ and Ⓛ, which correspond to the H-arm and the E-arm of a conventional waveguide magic-T. The magic-T couples the RF signal in-phase, and the LO signal out-of-phase to the two diode circuits. Matching between the magic-T and the diode circuits is accomplished by the slotlines. The IF signal is derived from port Ⓘ. The low-pass filter is connected to the IF port in order to suppress undesired signals.

III. Magic-T

To make double-balanced mixers, 90° or 180° four-port hybrids such as a branch line hybrid, parallel coupled line hybrid, a rat-rate, or a magic-T are required. These circuits are easily fabricated on a substrate and are applied to various types of balanced mixers. This section describes a *K*-band MIC magic-T with good isolation characteristics.

The configuration of the magic-T is shown in Fig. 2. This circuit is constructed with microstrip lines, slotlines and coupled slotlines. The magic-T is characterized by its special four-port configuration, that is, the two ports Ⓗ and Ⓔ, which correspond respectively to the H-arm and the E-arm of an ordinary wave-guide magic-T, are located on the same side opposite the other two-ports ① and ②. This port location has a significant advantage for practical applications, because this makes it possible to produce balanced-type mixers with no crossing of transmission lines. Crossing of lines is not suitable for a MIC structure, because it needs additional bonding and causes signal leakage which degrades the characteristics of balanced-type mixers.

0018-9480/80/0300-0180$00.75 ©1980 IEEE

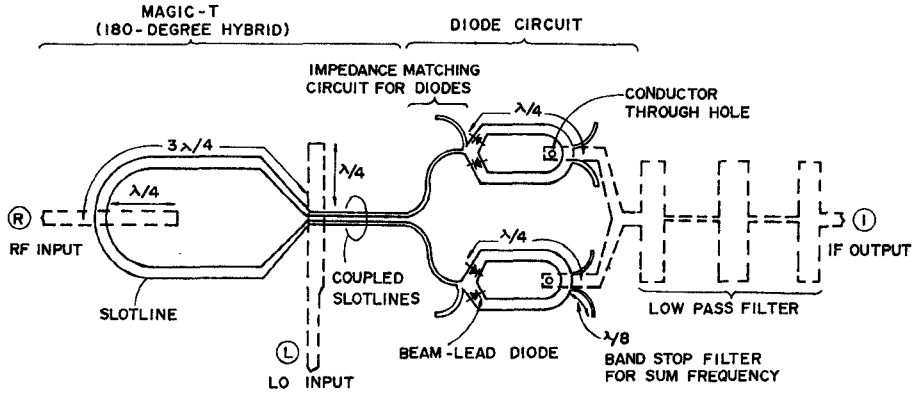

Fig. 1. Configuration of double-balanced mixer, where solid lines are slotlines and coupled slotlines on the substrate, dotted lines are microstrip lines on the reverse side of the substrate.

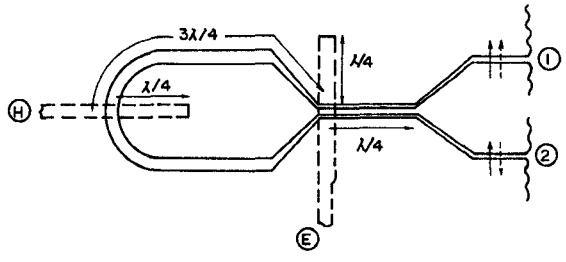

Fig. 2. Configuration of *K*-band MIC magic-T, where solid arrows and dotted arrows are schematic electric fields for the even-mode and the odd-mode of coupled slotlines, respectively.

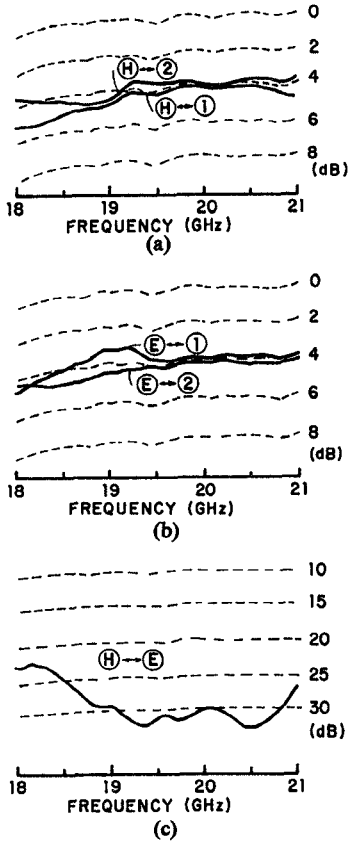

Fig. 3. Performance of MIC magic-T. (a) In-phase coupling characteristics. (b) Out-of-phase coupling characteristics. (c) Isolation characteristics.

The magic-T utilizes two orthogonal modes (even-mode and odd-mode [11]) of coupled slotlines. The signals fed into ports Ⓔ and Ⓗ are converted into the even-mode and the odd-mode, respectively. Thereafter, these signals are derived from ports ① and ②. The electric fields for the even-mode and the odd-mode are represented by solid arrows and dotted arrows in Fig. 2. Isolation between ports Ⓔ and Ⓗ is accomplished as follows: The signal from port Ⓗ is not coupled to the microstrip line of port Ⓔ because of the orthogonal characteristic of the coupled slotlines mode. On the other hand, for the signal from port Ⓔ, the three-quarter wavelength slotlines which facilitate matching of port Ⓔ behave as short-circuited stubs. Thus the signal from port Ⓔ is not propagated to port Ⓗ, because the signal is short-circuited at the intersection of the slotlines with the microstrip line port Ⓔ.

The magic-T is fabricated on a 0.3-mm thick alumina substrate with a center frequency of 20 GHz. To measure the performance of a magic-T, waveguide to microstrip transitions were necessary because the experimental equipment consisted of waveguide circuits. The waveguide to microstrip transition in this experiment is a ridged waveguide type [12], having six quarter-wave sections. Ports ① and ② are connected to microstrip lines using microstrip to slotline transitions, each having a quarter-wavelength. The insertion loss of the waveguide to microstrip transition is less than 0.2 dB and the return loss is greater than 20 dB in the 18- to 20.5-GHz band. Fig. 3 shows the experimental results of the MIC magic-T. In Fig. 3, dotted lines indicate the reference power level. The in-phase and out-of-phase coupling characteristics shown in Fig. 3(a) and (b), have some frequency sensitivity due to the effect of the waveguide to microstrip transitions. The couplings between Ⓗ↔①, ②, and Ⓔ↔①, ② are 4.0±0.8 dB over a range of 19–21 GHz and 4.0±0.4 dB in the 19.5- to 20.5-GHz band. The isolation between port Ⓗ and port Ⓔ is greater than 20 dB over a range of 18 to 21.0 GHz and greater than 30 dB in the 19- to 20.5-GHz band.

IV. Diode Circuit

As shown in Fig. 1, the diode circuit of the MIC double-balanced mixer consists of two impedance-matching circuits, four quarter-wavelength slotlines, two pairs of beam-lead Schottky-barrier diodes, two cylindrical conductors with a diameter of 0.5 mm, and a microstrip line. The equivalent diode circuit without the impedance matching circuit is shown in Fig. 4. In this figure four quarter-wavelength slotlines (S1), (S2), (S3), and (S4) act as short-circuited stubs for the LO and RF signals because these signals are short-circuited at the point directly below the microstrip lines which are connected to port (I). In this type of double-balanced mixer these quarter-wavelength slotlines are used to utilize effectively the RF and LO powers fed to the diodes. The basic principle of the mixer is described as follows:

When the RF and LO powers are fed into the diodes, total current appearing at port (I), port (R) and port (L) is expressed as follows (see Appendix):

$$\begin{aligned} i_{(I)}(t) = {} & 4\alpha i_s V_{RF} I_1(\alpha V_{LO})\cos(\omega_{LO}-\omega_{RF})t \\ & + 4\alpha i_s V_{RF} I_1(\alpha V_{LO})\cos(\omega_{LO}+\omega_{RF})t \\ & + 4\alpha i_s V_{RF} I_3(\alpha V_{LO})\cos(3\omega_{LO}-\omega_{RF})t \\ & + \cdots \end{aligned} \tag{1}$$

$$\begin{aligned} i_{(R)}(t) = {} & 4\alpha i_s V_{RF} I_0(\alpha V_{LO})\cos\omega_{RF}t \\ & + 4\alpha i_s V_{RF} I_2(\alpha V_{LO})\cos(2\omega_{LO}-\omega_{RF})t \\ & + 4\alpha i_s V_{RF} I_2(\alpha V_{LO})\cos(2\omega_{LO}+\omega_{RF})t \\ & + 4\alpha i_s V_{RF} I_4(\alpha V_{LO})\cos(4\omega_{LO}-\omega_{RF})t \\ & + \cdots \end{aligned} \tag{2}$$

$$\begin{aligned} i_{(L)}(t) = {} & 4\alpha i_s V_{LO}[I_0(\alpha V_{LO}) + I_2(\alpha V_{LO})]\cos\ {}_{LO}t \\ & + 4\alpha i_s V_{LO}[I_2(\alpha V_{LO}) + I_4(\alpha V_{LO})]\cos 3\ {}_{LO}t \\ & + 4\alpha i_s V_{LO}[I_4(\alpha V_{LO}) + I_6(\alpha V_{LO})]\cos 5\ {}_{LO}t \\ & + \cdots \end{aligned} \tag{3}$$

where

- α diode slope parameter,
- V_{RF} amplitude of the RF signal which is applied to each diode,
- V_{LO} amplitude of the LO signal which is applied to each diode,
- ω_{RF} RF angular frequency($=2\pi f_{RF}$),
- ω_{LO} LO angular frequency($=2\pi f_{LO}$),
- I_k modified Bessel function of the first kind of order k.

From (1), it can be seen that the total current at port (I) only contains frequency terms $mf_{LO} \pm f_{RF} (m \neq 0)$, when m is an odd integer. From (2) and (3), it can be seen that the frequency terms $mf_{LO} \pm f_{RF}$, where m is an even integer, and the fundamental RF signals appear at port (R), and the fundamental and odd harmonics of the LO signal appear at port (L).

Thus the IF, sum frequency and harmonic sidebands ($mf_{LO} \pm f_{RF}$; m = odd integer) are obtained at port (I). The image frequency signal does not appear at port (I) and port (L) but at port (R). Therefore, the band stop filters constructed at the eighth-wavelength slotlines, as shown in Fig. 1, are connected to the slotlines in order to suppress the sum frequency. A five-section low-pass filter [13] formed by the microstrip line is also connected to the IF port in order to suppress those undesired harmonics. The cutoff frequency of the filter is 8 GHz. In this type of double-balanced mixer it is comparatively easy to reactively terminate the image signal if the LO frequency is far from the RF frequency.

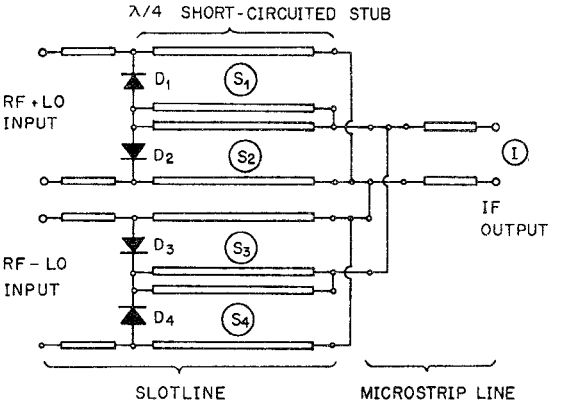

Fig. 4. Equivalent circuit of diode circuit.

The impedance of the beam-lead diode[1] is measured by a network analyzer, using the waveguide to microstrip transition mentioned in Section III. GaAs Schottky barrier diodes used here have a typical series resistance of 2.5 Ω, a junction capacitance of 0.05 pF at zero bias, a stray capacitance of 0.05 pF and an ideality factor of 1.17. The RF impedance of the diode at 20 GHz is $20 - j40$ (Ω), when the bias current is 0.5 mA at which the minimum conversion loss is obtained. The impedance-matching circuit for the diode is designed as shown in Fig. 1 using a quarter-wavelength impedance transformer and a short-circuited stub connected in series to the slotline in order to cancel the capacitance of diodes. It is noteworthy that short- or open-circuited stubs can be easily connected to the slotline. This configuration of the matching circuit is suitable for adjusting integrated circuits, because the stub length can be easily changed by bonding with gold wires or ribbons.

V. Experimental Results

The double-balanced mixer shown in Fig. 1 is fabricated by a photolithographic technique on a 0.3-mm thick alumina substrate with a relative permittivity of 9.6. A 500-Å thick nickel-chromium and 6000-Å thick gold are deposited on the substrate by a vacuum evaporation method. Fig. 5 shows photographs of the mixer pattern. In Fig. 5(a) is the pattern of the microstrip line on the reverse side of the substrate and Fig. 5(b) is the pattern of a slotline and coupled slotlines on the substrate. The gold thickness of the microstrip lines and slotlines in this

[1] V558 of NEC

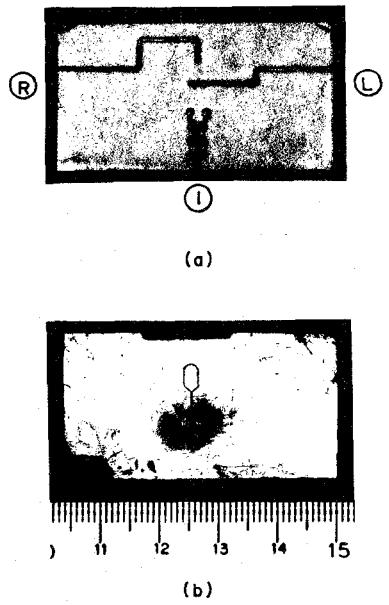

Fig. 5. Photograph of double-balanced mixer. (a) Microstrip pattern on the reverse substrate. (b) Slotline pattern.

circuit is 3 μm, which is electrically plated after the photoetching process. A top view of the entire integrated mixer is shown in Fig. 6, including the waveguide to microstrip transitions at the RF and LO ports and the coaxial connector at the IF port. The microstrip pattern can be seen in this photograph.

The measured conversion losses of the mixer are presented in Fig. 7 for several LO frequencies. These losses include the insertion loss, that is, 0.2 dB of waveguide to microstrip transition and 0.5 dB of low-pass filter. As can be seen in Fig. 7, the minimum conversion loss attained at a signal frequency of 19.6 GHz is 4.7 dB. The cause for some frequency sensitivities in conversion loss is probably the positional inaccuracy of the holes on the substrate and the bonded diodes on the slotlines. Another reason is that four diodes used here are not completely matched. The isolation between ports Ⓛ and Ⓡ is greater than 20 dB, and between ports Ⓛ and Ⓘ greater than 30 dB, as shown in Fig. 8. As described above, the double-balanced mixer used for the 20-GHz band has good isolation between the three ports in addition to a low conversion loss, due to the effective combination of microstrip lines, slotlines, coupled slotlines and two pairs of Schottky-barrier diodes.

VI. Conclusion

A new MIC double-balanced mixer has been successfully developed, which is suitable for high frequencies up to the millimeter-wave bands. This mixer consists of an MIC magic-T and a diode circuit. These circuits are constructed by using combinations of microstrip lines, slotlines, coupled slotlines and beam-lead diodes. The coupling characteristics of the magic-T are typically 4 dB between 19 and 21 GHz and isolation is greater than 20 dB in the 18- to 21-GHz range. The minimum conversion loss of the mixer is 4.7 dB at a signal frequency of 19.6 GHz, and isolation between the three ports is greater than 20 dB in the 18- to 21-GHz range. This type of double-balanced mixer can be made without crossing transmission lines, and its configuration is very suitable for the beam-lead diode. The signals appearing at port Ⓘ are the IF signal and the harmonic sidebands. The image signal does not appear at port Ⓘ or port Ⓛ, but does appear at port Ⓡ. This mixer can be easily fabricated using ordinary MIC techniques and can be applied to other

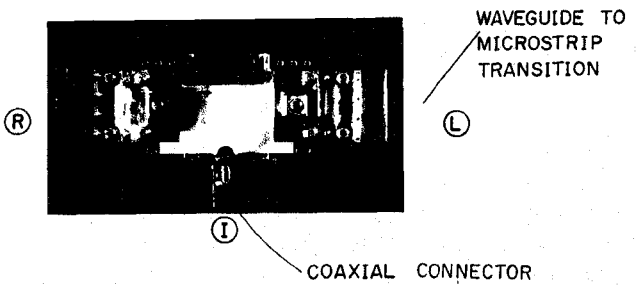

Fig. 6. Top view of an entire double-balanced mixer.

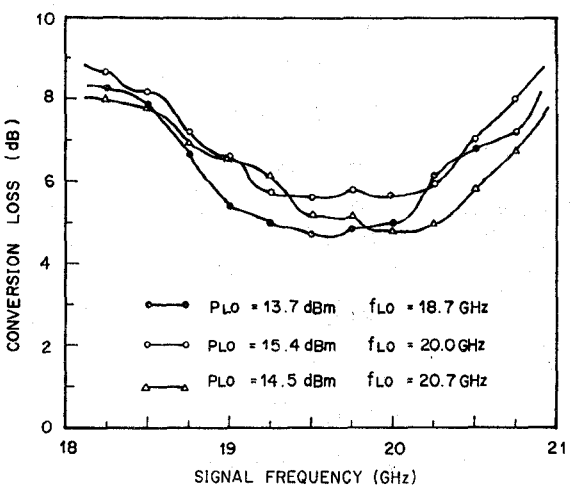

Fig. 7. Conversion loss of double-balanced mixer.

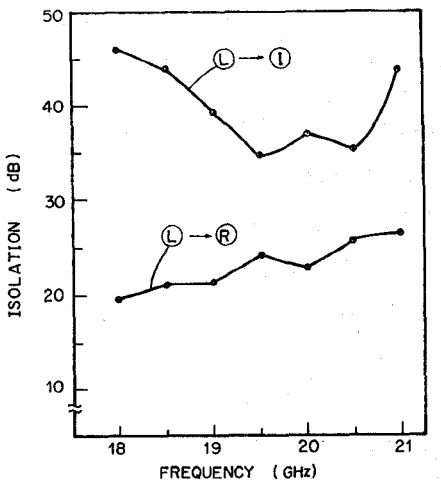

Fig. 8. Isolation characteristics of double-balanced mixer.

balanced type devices, such as balanced modulators and balanced upconverters.

APPENDIX

Equations (1)–(3) are derived as follows [14]–[16].

Fig. 9 shows the schematic circuit for illustrating the signal flow around the diodes. In this figure, the four quarter-wavelength slotlines in Fig. 4 is regarded as two coplanar lines for the current appearing at port ①. In Fig. 9, when the voltage V is fed into diodes D_1, D_2, D_3, and D_4, the instantaneous currents passing through diodes i_1, i_2, i_3, and i_4 are written in the usual expressions.

$$i_1 = -i_s(e^{-\alpha V}-1) \tag{4}$$

$$i_2 = i_s(e^{\alpha V}-1) \tag{5}$$

$$i_3 = i_s(e^{\alpha V}-1) \tag{6}$$

$$i_4 = -i_s(e^{-\alpha V}-1) \tag{7}$$

where α is the diode slope parameter and i_s is the saturation current. From (4)–(7), the differential conductance for each diode is expressed as follows:

$$g_1 = di_1/dV = \alpha i_s e^{-\alpha V} \tag{8}$$

$$g_2 = di_2/dV = \alpha i_s e^{\alpha V} \tag{9}$$

$$g_3 = di_3/dV = \alpha i_s e^{\alpha V} \tag{10}$$

$$g_4 = di_4/dV = \alpha i_s e^{-\alpha V} \tag{11}$$

We assume that the conductance of the diodes is modulated with periodic signals

$$V = V_{LO}\cos\omega_{LO}t, \qquad \text{for } D_1 \text{ and } D_2 \tag{12}$$

$$V = V_{LO}\cos(\omega_{LO}t+\pi), \qquad \text{for } D_3 \text{ and } D_4 \tag{13}$$

where $\omega_{LO}=2\pi f_{LO}$ is LO angular frequency and V_{LO} is the amplitude of the LO signal applied to each diode. The conductances of the diodes are expressed as follows:

$$g_1(t) = \alpha i_s \exp[-\alpha V_{LO}\cos\omega_{LO}t] \tag{14}$$

$$g_2(t) = \alpha i_s \exp[\alpha V_{LO}\cos\omega_{LO}t] \tag{15}$$

$$g_3(t) = \alpha i_s \exp[\alpha V_{LO}\cos(\omega_{LO}t+\pi)] \tag{16}$$

$$g_4(t) = \alpha i_s \exp[-\alpha V_{LO}\cos(\omega_{LO}t+\pi)]. \tag{17}$$

Furthermore, the RF signal

$$v = V_{RF}\cos\omega_{RF}t \tag{18}$$

is fed into the above differential conductances, where $\omega_{RF}=2\pi f_{RF}$ is RF angular frequency and V_{RF} is the amplitude of the RF signal applied to each diode. From the instantaneous currents passing through the diodes, $i_{12}(t)$ and $i_{34}(t)$ are expressed as follows:

$$\begin{aligned} i_{12}(t) &= i_2(t)-i_1(t) \\ &= 2\alpha i_s \sinh[\alpha V_{LO}\cos\omega_{LO}t] \\ &\quad \cdot [V_{LO}\cos\omega_{LO}t + V_{RF}\cos\omega_{RF}t] \\ &= 2\alpha i_s V_{LO} I_1(\alpha V_{LO}) \\ &\quad + 2\alpha i_s V_{LO}[I_1(\alpha V_{LO}) + I_3(\alpha V_{LO})]\cos 2\omega_{LO}t \\ &\quad + 2\alpha i_s V_{RF} I_1(\alpha V_{LO})\cos(\omega_{LO}-\omega_{RF})t \\ &\quad + 2\alpha i_s V_{RF} I_1(\alpha V_{LO})\cos(\omega_{LO}+\omega_{RF})t \\ &\quad + 2\alpha i_s V_{LO}[I_3(\alpha V_{LO}) + I_5(\alpha V_{LO})]\cos 4\omega_{LO}t \\ &\quad + 2\alpha i_s V_{RF} I_3(\alpha V_{LO})\cos(3\omega_{LO}-\omega_{RF})t + \cdots \end{aligned} \tag{19}$$

$$\begin{aligned} i_{34}(t) &= i_3(t)-i_4(t) \\ &= 2\alpha i_s \sinh[\alpha V_{LO}\cos(\omega_{LO}t+\pi)] \cdot [V_{LO}\cos(\omega_{LO}t+\pi) \\ &\quad + V_{RF}\cos\omega_{RF}t] \\ &= 2\alpha i_s V_{LO} I_1(\alpha V_{LO}) \\ &\quad + 2\alpha i_s V_{LO}[I_1(\alpha V_{LO}) + I_3(\alpha V_{LO})]\cos(2\omega_{LO}t+2\pi) \\ &\quad + 2\alpha i_s V_{RF} I_1(\alpha V_{LO})\cos(\omega_{LO}t-\omega_{RF}t+\pi) \\ &\quad + 2\alpha i_s V_{RF} I_1(\alpha V_{LO})\cos(\omega_{LO}t+\omega_{RF}t+\pi) \\ &\quad + 2\alpha i_s V_{LO}[I_3(\alpha V_{LO}) + I_5(\alpha V_{LO})]\cos(4\omega_{LO}t+4\pi) \\ &\quad + 2\alpha i_s V_{RF} I_3(\alpha V_{LO})\cos(3\omega_{LO}t-\omega_{RF}t+\pi) \\ &\quad + \cdots. \end{aligned} \tag{20}$$

Total current expression at port ① is

$$\begin{aligned} i_{①}(t) &= i_{12}(t)-i_{34}(t) \\ &= 4\alpha i_s V_{RF} I_1(\alpha V_{LO})\cos(\omega_{LO}-\omega_{RF})t \\ &\quad + 4\alpha i_s V_{RF} I_1(\alpha V_{LO})\cos(\omega_{LO}+\omega_{RF})t \\ &\quad + 4\alpha i_s V_{RF} I_3(\alpha V_{LO})\cos(3\omega_{LO}-\omega_{RF})t \\ &\quad + \cdots. \end{aligned} \tag{21}$$

In (19) and (20), the following formula is used:

$$\sinh(Z\cos\theta) = 2\sum_{k=0}^{\infty} I_{2k+1}(Z)\cos(2k+1)\theta \tag{22}$$

where I_k are modified Bessel functions of the first kind of order k.

It can be seen that the total current at port ① only contains frequency terms $mf_{LO}\pm f_{RF}(m\neq 0)$, where m is an odd integer.

In Fig. 9 sum current i_1+i_2 and i_3+i_4 flow toward the magic-T. These currents do not appear at port ①, but appear at port ® or port Ⓛ. These currents are expressed as follows:

$$\begin{aligned} i'_{12}(t) &= i_1(t)+i_2(t) \\ &= 2\alpha i_s \cosh[\alpha V_{LO}\cos\omega_{LO}t] \\ &\quad \cdot [V_{LO}\cos\omega_{LO}t + V_{RF}\cos\omega_{RF}t] \end{aligned}$$

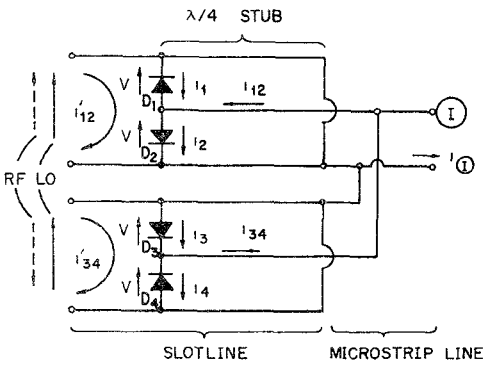

Fig. 9. Schematic circuit of Fig. 4.

$$
\begin{aligned}
&= 2\alpha i_s V_{LO}[I_0(\alpha V_{LO}) + I_2(\alpha V_{LO})]\cos\omega_{LO}t \\
&\quad + 2\alpha i_s V_{RF} I_0(\alpha V_{LO})\cos\omega_{RF}t \\
&\quad + 2\alpha i_s V_{LO}[I_2(\alpha V_{LO}) + I_4(\alpha V_{LO})]\cos 3\omega_{LO}t \\
&\quad + 2\alpha i_s V_{RF} I_2(\alpha V_{LO})\cos(2\omega_{LO} - \omega_{RF})t \\
&\quad + 2\alpha i_s V_{RF} I_2(\alpha V_{LO})\cos(2\omega_{LO} + \omega_{RF})t \\
&\quad + 2\alpha i_s V_{RF} I_4(\alpha V_{LO})\cos(4\omega_{LO} - \omega_{RF})t \\
&\quad + \cdots . \qquad (23)
\end{aligned}
$$

$$
\begin{aligned}
i'_{34}(t) &= i_3(t) + i_4(t) \\
&= 2\alpha i_s \cosh[V_{LO}\cos(\omega_{LO}t + \pi)] \cdot [V_{LO}\cos(\omega_{LO}t + \pi) \\
&\quad + V_{RF}\cos\omega_{RF}t] \\
&= 2\alpha i_s V_{LO}[I_0(\alpha V_{LO}) + I_2(\alpha V_{LO})]\cos(\omega_{LO}t + \pi) \\
&\quad + 2\alpha i_s V_{RF} I_0(\alpha V_{LO})\cos\omega_{RF}t \\
&\quad + 2\alpha i_s V_{LO}[I_2(\alpha V_{LO}) + I_4(\alpha V_{LO})]\cos(3\omega_{LO}t + 3\pi) \\
&\quad + 2\alpha i_s V_{RF} I_2(\alpha V_{LO})\cos(2\omega_{LO}t - \omega_{RF}t + 2\pi) \\
&\quad + 2\alpha i_s V_{RF} I_2(\alpha V_{LO})\cos(2\omega_{LO}t + \omega_{RF}t + 2\pi) \\
&\quad + 2\alpha i_s V_{RF} I_4(\alpha V_{LO})\cos(4\omega_{LO}t - \omega_{RF}t + 4\pi) \\
&\quad + \cdots . \qquad (24)
\end{aligned}
$$

In (23) and (24), the following formula is also used.

$$
\cosh(Z\cos\theta) = I_0(Z) + 2\sum_{k=1}^{\infty} I_k(Z)\cos 2k\theta . \qquad (25)
$$

From (23) and (24), the currents appearing at port Ⓡ and Ⓛ are expressed as follows:

$$
\begin{aligned}
i_{Ⓡ}(t) &= i'_{12}(t) + i'_{34}(t) \\
&= 4\alpha i_s V_{RF} I_0(\alpha V_{LO})\cos\omega_{RF}t \\
&\quad + 4\alpha i_s V_{RF} I_2(\alpha V_{LO})\cos(2\omega_{LO} - \omega_{RF})t \\
&\quad + 4\alpha i_s V_{RF} I_2(\alpha V_{LO})\cos(2\omega_{LO} + \omega_{RF})t \\
&\quad + 4\alpha i_s V_{RF} I_4(\alpha V_{LO})\cos(4\omega_{LO} - \omega_{RF})t \\
&\quad + \cdots . \qquad (26)
\end{aligned}
$$

$$
\begin{aligned}
i_{Ⓛ}(t) &= i'_{12}(t) - i'_{34}(t) \\
&= 4\alpha i_s V_{LO}[I_0(\alpha V_{LO}) + I_2(\alpha V_{LO})]\cos\omega_{LO}t \\
&\quad + 4\alpha i_s V_{LO}[I_2(\alpha V_{LO}) + I_4(\alpha V_{LO})]\cos 3\omega_{LO}t \\
&\quad + 4\alpha i_s V_{LO}[I_4(\alpha V_{LO}) + I_6(\alpha V_{LO})]\cos 5\omega_{LO}t \\
&\quad + \cdots . \qquad (27)
\end{aligned}
$$

It can be seen from (26) and (27) that the frequency terms $mf_{LO} \pm f_{RF}$, where m is an even integer, and the fundamental RF signal appear at port Ⓡ, and the fundamental and odd harmonics of the LO signal appear at port Ⓛ.

ACKNOWLEDGMENT

The authors wish to thank Dr. Yamamoto, Dr. Ohtomo, Dr. Akaike, and Dr. Kurita in Yokosuka Electrical Communication Laboratory for their encouragement and suggestions.

REFERENCES

[1] T. Araki and H. Hirayama, "A 20-GHz integrated balanced mixer" *IEEE Trans. Microwave Theory Tech.*, vol. MTT-19, pp. 638–643, July 1971.

[2] K. M. Johnson, "*X*-band integrated circuit mixer with reactively terminated image," *IEEE Trans. Microwave Theory Tech.*, vol. MTT-16, pp. 388–397, July 1968.

[3] L. E. Dickens and D. W. Maki, "An integrated-circuit balanced mixer, image and sum enhanced," *IEEE Trans. Microwave Theory Tech.*, vol. MTT-23, pp. 276–281, Mar. 1975.

[4] G. Begemann, "An X-band balanced fine-line mixer," *IEEE Trans. Microwave Theory Tech.*, vol. MTT-26, pp. 1007–1011, Dec. 1978.

[5] T. K. Hunton and T. S. Takeuchi, "Recent developments in microwave slotline mixers and frequency multipliers," in *1970 IEEE G-MTT Int. Symp. Dig. Tech. Papers*, pp. 196–199, May 1970.

[6] U. H. Gysel, "A 26.5-to-40-GHz planar balanced mixer," in *Proc. 5th European Microwave Conf.*, pp. 491–495, Sept. 1975.

[7] L. E. Dickens and D. W. Maki, "A new "phased-type" image enhanced mixer," in *1975 IEEE G-MTT Int. Symp. Digest Tech. Papers*, pp. 149–151, 1975.

[8] R. Pflieger, "A new MIC double-balanced mixer with RF and IF band overlap," in *1973 IEEE G-MTT Int. Sym. Digest Tech. Papers*, pp. 301–303, June 1973.

[9] M. Aikawa and H. Ogawa, "A new MIC magic-T using coupled slotlines," submitted to *IEEE Trans. Microwave Theory Tech.*, 1979.

[10] M. Aikawa and H. Ogawa, "2 Gb double-balanced PSK modulator using coplanar waveguides," in *1979 ISSCC Digest*, pp. 172–173, Feb. 1979.

[11] J. B. Knorr and K. D. Kuchler, "Analysis of coupled slots and coplanar strips on dielectric substrate," *IEEE Trans. Microwave Theory Tech.*, vol. MTT-23, pp. 541–548, July 1975.

[12] S. Hopfer, "The design of ridged waveguide," *IRE Trans. Microwave Theory Tech.*, vol. MTT-3, pp. 20–29, Oct. 1955.

[13] Matthaei, Young, and Jones, *Microwave Filters, Impedance-Matching Networks, and Coupling Structures*. New York: McGraw-Hill, 1964, pp. 83–104.

[14] M. R. Barber, "Noise figure and conversion loss of the Schottky-barrier diode," *IEEE Trans. Microwave Theory Tech.*, vol. MTT-15, pp. 629–635, Nov. 1967.

[15] M. V. Schneider and W. W. Snell, "Harmonically pumped stripline down-converter," *IEEE Trans. Microwave Theory Tech.*, vol. MTT-23, pp. 271–275, Mar. 1975.

[16] M. Cohn, J. E. Degnenford, and B. A. Newman, "Harmonic mixing with an antiparallel diode pair," *IEEE Trans. Microwave Theory Tech.*, vol. MTT-23, pp. 667–673, Aug. 1975.